

## 1. Publishable summary

The HISTORIC project aimed to design, develop and test digital photonic integrated circuits containing ultra-compact gates based on micro-ring or micro-disk lasers or photonic crystal lasers pumped either by current injection or by optical pumping, for use in e.g. all-optical packet switching for both datacom and telecom. The main motivation was to enhance the use of optics in switching and routing by developing small footprint, low power consumption and high speed photonic components.

We specifically planned to focus on highly functional photonic digital processing units for employment in innovative approaches towards optical packet or burst switching that promise improved performance with respect to electronic solutions. These buffers or processing units were to be implemented as complex photonic integrated circuits containing a large number of interconnected digital photonic elements.

The basic digital photonic elements envisaged were all-optical flip-flops and gates implemented using ultra-compact laser diodes. Owing to their very small size these devices can be switched rapidly with low pulse energies. Different ultra compact laser diodes were going to be investigated such as single or coupled micro-ring/micro-disk lasers and optically and electrically pumped photonic crystal lasers.

An example of the typical photonic digital processing units that was to be investigated is shown in Figure 1.1, a schematic of a 4x1 multiplexer/demultiplexer with latching memory. In this scheme, the gates on the left hand side act as optical time division demultiplexers (only passing the signal when a clock pulse opens the gate) and their outputs act as set pulses for the set-reset flip-flops in the central part. The gates on the right hand side just pass the output of the S-R flip-flop during each clock pulse. The S-R flip-flops together with these gates thus act as D-flip-flops.

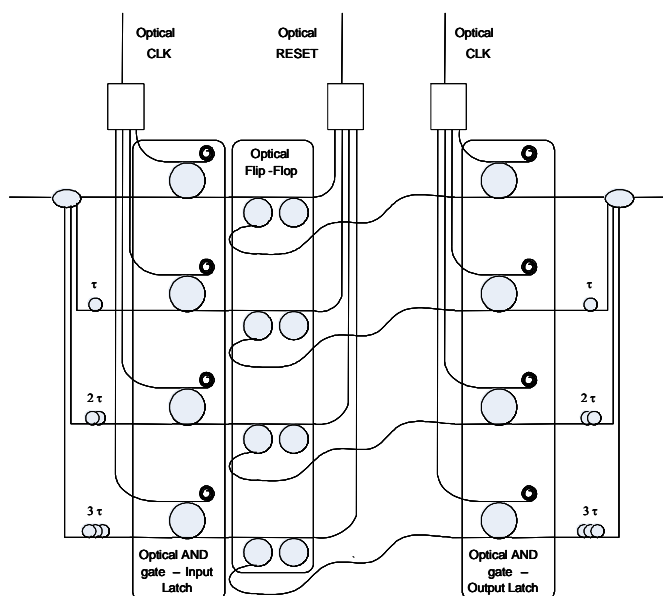


Figure 1.1: Illustration of a functional digital photonic circuit based on micro-disk laser diodes; in this case a 4x1 mux/demux with latching memory.

The optical flip-flops and gates are implemented as micro-disk lasers, but could also be implemented based on the other ultra-compact laser diodes which will be studied in this project. The gates will normally be lasers biased below threshold.

It was one of the main goals of the project to demonstrate that the silicon/III-V platform would enable the fabrication of much more complex PICs than has so far been possible. In addition, the project aimed to demonstrate that this ‘large scale integration’ could be used for the fabrication of PICs which allow circumventing some of the disadvantages currently associated with optical packet switching. In particular, essential functionalities such as buffering and synchronisation, which have so far been the main hurdle to the success of all-optical packet switching, were going to be tackled. It was hence expected that a much better understanding of the possibilities and potential of all-optical packet switching would result and that new insights in this domain would be gained.

Photonic packet switching could be a very interesting alternative for electronic packet switching at ultra high bitrates. However, photonic packet switching has been criticized for being less power efficient than electronic packet switching. Indeed, typical transistors are capable of switching with 1 fJ of energy per bit, while photonic switching (optical flip-flops e.g.) typically requires energies of the order of pJ per bit. Nevertheless, significant progress is possible in the area of photonic switching and much lower switching energies than 1 pJ per bit have already been demonstrated.

The project has 4 **technical workpackages**: System design and specifications (WP1), Micro-disk based devices and PICs (WP2), Advanced all-optical flip-flops (WP3), and System experiments and assessment (WP4).

The **total costs and funding** amount to 3,111,239 € and 2,300,00 €, respectively (Manpower: 259 PM including 10 PM for management).

The website of the project can be found at [www.ict-historic.eu](http://www.ict-historic.eu).



For more information, please contact the project coordinator

Prof. Geert Morthier

Photonics Research Group, Department of Information Technology, IMEC-Ghent University,  
Sint-Pietersnieuwstraat 41, B-9000 Ghent, Belgium

E-mail: [Geert.Morthier@intec.UGent.be](mailto:Geert.Morthier@intec.UGent.be), Tel. +32 9 2648934

### Main results achieved so far

In the first year, the first all-optical flip-flops based on heterogeneously integrated InP microdisk lasers have been demonstrated with excellent performance. Disk lasers with diameters as small as  $7.5\ \mu\text{m}$  have been switched between clockwise and counterclockwise unidirectional operation. These were the all-optical flip-flops with the smallest footprint of the active device. The InP microdisk lasers are coupled to silicon wire waveguides, which are themselves coupled to single mode fiber using grating couplers. Unidirectional operation was obtained for DC currents as low as  $1.75\ \text{mA}$ , corresponding with a total power consumption of less than  $3\ \text{mW}$ , and with extinction ratios of  $12\text{-}15\ \text{dB}$ . Switching energies as low as  $1.8\ \text{fJ}$  have also been obtained using  $100\ \text{ps}$  long switching pulses. Maximum output powers are over  $40\ \mu\text{W}$ , which implies that the flip-flops have a fan-out larger than 2.

In the second year, we also investigated the deposition of a thin silica layer on top of the InP, to improve the heat sinking. We found that in addition, this silica deposition also improves the bonding yield significantly, to close to 100%. We also started investigating the fabrication of microdisk lasers without tunnel junctions, but with the lossy InGaAs top contact layer being etched away at the edge, above the whisperin gallery mode. Initial bonding with this epi-layer occurred under stress and we suspected this was the reason for obtaining cracks in the InP during further processing.

In the final year and a half of the project, we still struggled with the bad quality of the epi-material with tunnel junctions. We purchased a wafer with tunnel junctions from another vendor, but devices fabricated using this InP-stack exhibited very high series resistance, which also prevented lasing operation. Nevertheless, using what seems to be better epi (with tunnel junctions) that was delivered to partner TUE, we managed recently to fabricate 3 samples with good devices. The L-I curve of a  $7.5\ \mu\text{m}$  diameter microdisk is shown in Figure 1.2. It shows again a low threshold of  $0.4\ \text{mA}$  and a unidirectional behaviour as can be clearly seen. We also significantly reduced the series resistance by choosing for a thicker bottom contact layer and a new contact recipe. The thicker bottom contact layer is moreover expected to lead to better heat sinking.

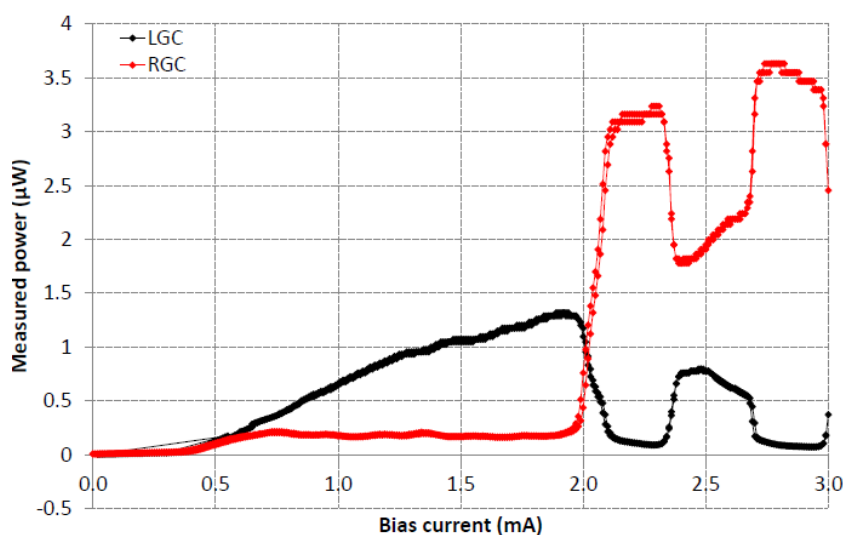


Figure 1.2: L-I characteristic of a recently fabricated microdisk laser.

In the final phase of the project, we perfected the fabrication processes even further. The use of EBL was further developed for the definition of the top contact, such that overlap of the contact metal with the WGM is minimal. We also investigated machine bonding to obtain a better reproducibility and controllability of the bonding layer thickness, as well as the deposition of a thin alumina layer (instead of a silica layer) on top of the InP to further improve the heat sinking. Alumina has a higher thermal conductivity than silica. Bonding with this oxide on InP went very well (with a similar yield as for silica) and first devices have been processed. However, there were some problems with the etching preventing the lasing of these devices.

Other means to optimise the performance of microdisk lasers were also identified, but not yet tested. E.g. better confinement and thus smaller disk diameters would be possible replacing the BCB surrounding the disk by a lower index polymer. BCB has a refractive index of more than 1.55, while polymers for optical applications are available with a refractive index of 1.3. We also looked for and found polymers with higher thermal conductivity than BCB to surround the microdisks, something which would result in even better heat sinking. Both polymers are ordered, and their use for the microdisk fabrication (e.g. compatibility with the rest of the processing) will be explored after the completion of the HISTORIC project.

In spite of the problems with the epi-material, several functions were demonstrated using samples with microdisk lasers that became available earlier in the project and were donated by the WADIMOS project. In addition to the set-reset flip-flops, several other logic (and optical signal processing) building blocks have been designed using microdisk lasers. We started with the demonstration of single disks as gates/wavelength converters and time domain demultiplexers. It was found that these functions can be performed using microdisk lasers without requiring electrical bias (i.e. without current injection nor the appliance of negative voltage). The principle is in all cases the same, a ‘low power’ probe and a ‘high power’ pump are biased near a different resonance of the microdisk resonator. The ‘high power’ pump pulses are absorbed in the InP microdisk where they create charge carriers, which in turn change the refractive index and therefore shift the resonance wavelength for the ‘low power’ probe signal. Experiments reveal that the switching obtained in this manner is quite fast. As shown in Figure 1.3, we obtained typical rise and fall time of 18.6 and 26.4 ps respectively, implying an achievable gating and all-optical wavelength conversion speed beyond 20Gbps. This was obtained using pump pulses with an energy of 180fJ and since no bias is required, this is the total energy consumption per bit. Experiments at 10Gbit/s with a pseudo random bit sequence allowed gating/wavelength conversion with a bit-error-rate below  $10^{-9}$ , and a power penalty of 4dB. It is expected that even higher bitrates (up to 40Gbit/s) would be possible by using ion implantation in the disks, the injection of a holding beam or a reduced extinction ratio for the pump signal in order to reduce the carrier lifetime further.

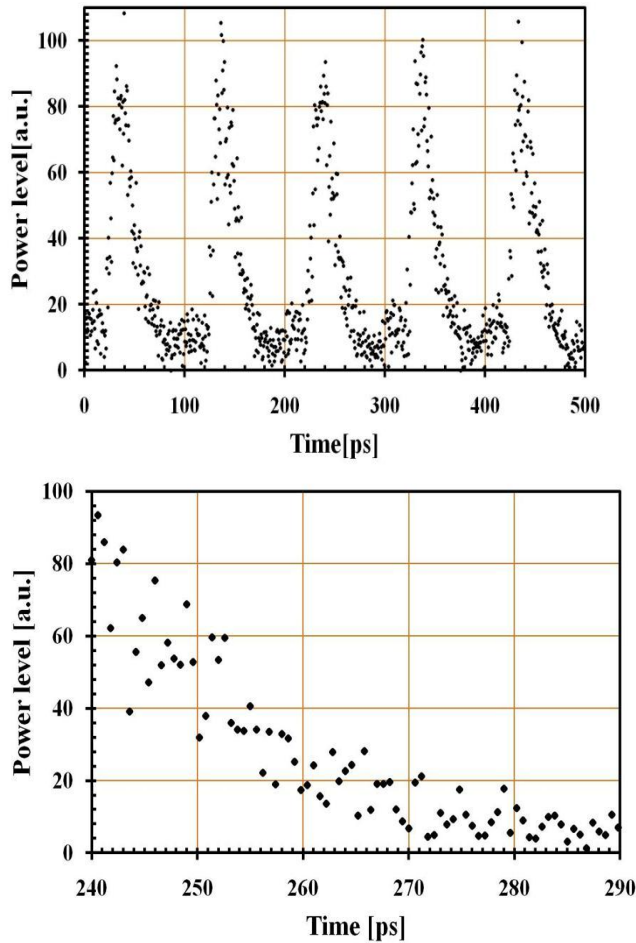


Figure 1.3: Output waveform after all-optical gating with 8ps long pulses (a) and falling (b) transient details.

Very recently, we also found through numerical simulations that microdisks biased just below threshold can also operate as a sort of optical, resonant isolator. The physical effect which makes such isolation possible is the same as that allowing a stable unidirectional operation in disk and ring lasers: the difference between self gain suppression (i.e. the suppression of the gain of e.g. the CW mode caused by the CW power) and the cross gain suppression (i.e. the suppression of the gain of e.g. the CCW mode caused by the CW power). The isolation can typically be obtained in a configuration as shown in the l.h.s. of Figure 1.4, in which the disk laser is biased very close to the threshold current. If the injected power  $P_1$  is much larger than the reflected power  $P_3$ , then the asymmetric gain suppression will result in a smaller gain for the clockwise (CW) propagating field (thus for  $P_3$ ) and if the gain is close to the threshold gain, the transmittance  $P_2/P_1$  will be much larger than the transmittance  $P_4/P_3$ . The obtained isolation is shown on the r.h.s. of Figure 1.4. It can be noticed that the highest isolation is obtained for input powers which correspond with the typical output power of fabricated microdisk lasers. The isolation has so far not been demonstrated experimentally, mainly due to the lack of good microdisk lasers coupled to two bus waveguides as in Figure 1.4. Such an isolator type would be of great use in the design of more complicated photonic integrated circuits, where backreflections and signals leaking from components further down the logic chain have to be suppressed. The potential of isolation, fan-out, cascability and signal refreshing are key requirements for building blocks of logic systems.

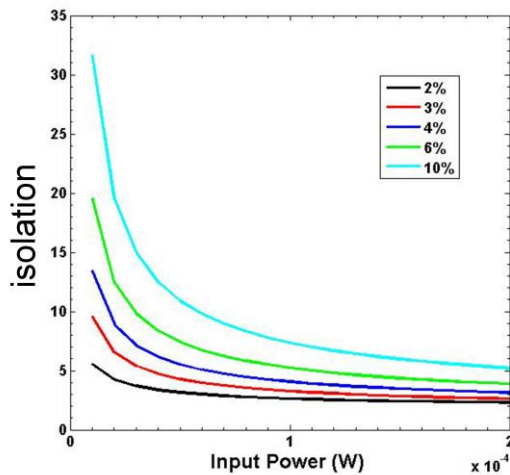
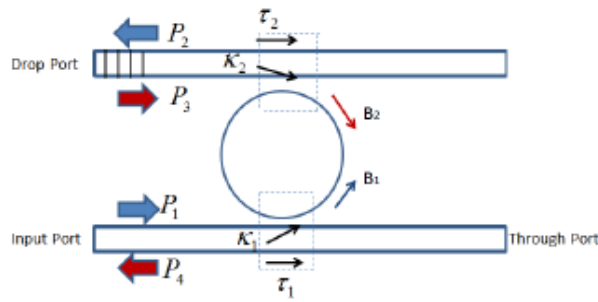


Figure 1.4: Schematic of a resonant isolator based on a microdisk laser (lhs) and numerically obtained isolation vs. input power (rhs).

In addition to all-optical functions, the use as transmitter and photodetector for optical interconnect was explored. The direct modulation of microdisk lasers showed high bandwidth under injection locking. Error-free 10Gb/s operation was obtained for a bias current of only 0.75mA and a modulation signal of 350mV, with an extinction ratio of 6.2dB. 20Gb/s operation was obtained with a BER below  $10^{-6}$  and an extinction ratio of only 1.65dB, but it is expected that this can be further improved. In addition to direct modulation, the disks can be operated in the carrier-depletion regime as external modulators. Again, 10 Gb/s operation with a BER below  $10^{-11}$  was demonstrated. BER measurements at 2.5, 5 and 10Gb/s are shown in Figure 1.5 and compared to the results obtained with a commercial modulator. The energy consumption is 36fJ/bit which is comparable to state-of-the-art modulators. The required drive voltage of 1.625V is compatible with state-of-the-art BiCMOS technologies and is lower than that needed in alternative modulator concepts, such as Silicon based Mach-Zehnder modulators.

The microdisks were also demonstrated as resonant photodetectors with a sensitivity of 0.3A/W, limited by the waveguide to disk coupling. An open eye up to 2Gb/s could be obtained. In this case, only one epitaxial layer is needed for lasing and detection and the devices can be structured in the same lithography. Improved devices, with better waveguide to disk coupling are currently under fabrication.

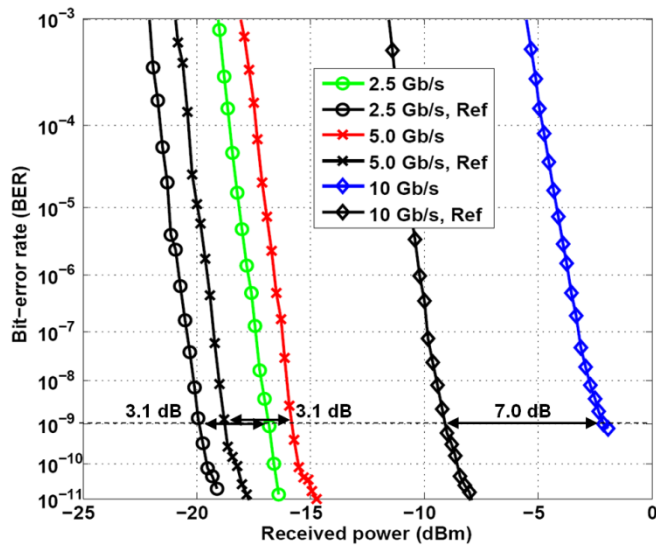


Figure 1.5: BER measurements of the InP microdisk modulator and a commercial modulator at 2.5, 5 and 10 Gb/s.

For the photonic crystal lasers, two paths were explored from the beginning of the project: one with optical pumping and one with electrical pumping. Progress on the optically pumped photonic crystal lasers was first of all focussed on the optimisation of the coupling between the silicon waveguide and the InP membrane. This resulted in laser operation for a threshold pump power of  $17\mu\text{W}$ , as can be seen in Figure 1.6. A lot of effort was also devoted to obtaining robust CW operation of the hybrid nanolasers by fully encapsulating them into SiO<sub>2</sub> in order to decrease the overall thermal resistance.

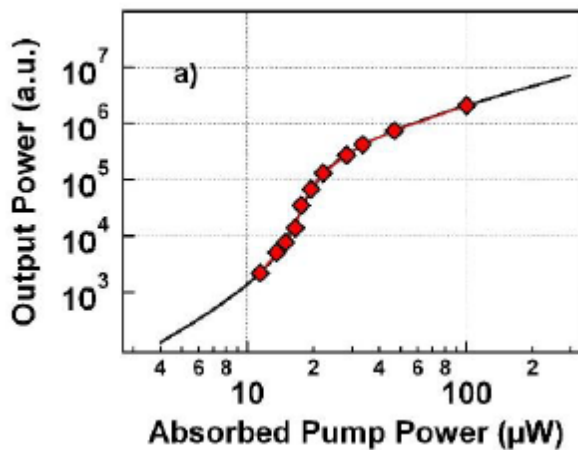


Figure 1.6: Laser characteristics of the optically pumped photonic crystal laser.

Finally, bistable switching, i.e. flip-flop operation, was demonstrated using these structures. Switching energies of  $0.4\text{fJ}$  were measured with switching speeds below  $50\text{ps}$ . Figure 1.7 shows the bistable characteristics under optical injection as a function of the detuning.

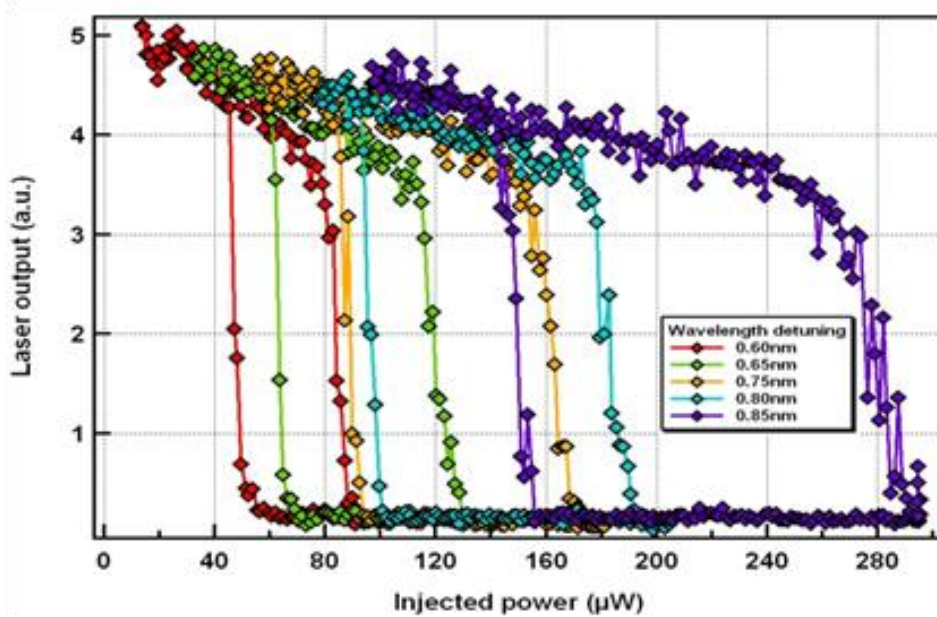


Figure 1.7: Bistable characteristics of the photonic crystal lasers for different detuning of the injected beam.

For the electrically injected photonic crystal lasers, the processes for obtaining highly resistive oxidized Al containing layers have been optimised. A series resistance of these resistive layers of at least 100k $\Omega$  has been obtained, 3 orders of magnitude higher than before oxidation. The cause of the blue shift in the PL spectrum has been identified as quantum well intermixing due to dry etching. Hence, it can be avoided by using wet etching. Finally, a W1-like cavity has been chosen for the laser structure and its tolerance to alignment error and hole radius variation has been analysed using FDTD software. Taking into account the maximum variations for e-beam lithography, an acceptable Q-factor is still obtained.

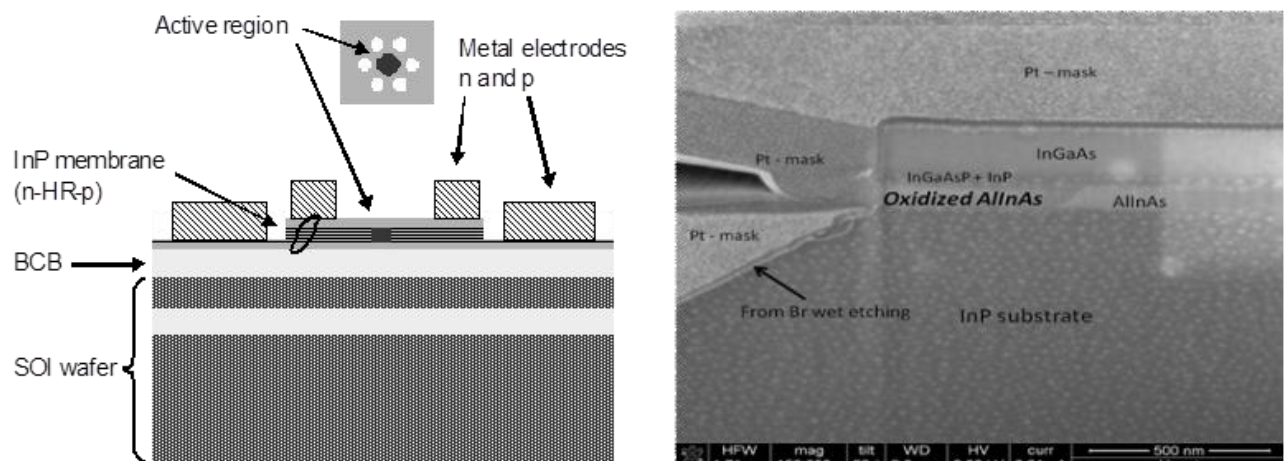


Figure 1.8: left: schematic view of the PhC laser , right: SEM picture of the AlInAs oxide.

Fabrication of this electrically injected photonic crystal laser is still on-going. TUE has developed a full process scheme in collaboration with the PHILIPS company. But only the first and second regrowth are finished, which are the regrowth of the InGaAsP layer for submicron active integration and of the AlInAs layer for the current blocking function.